

## Reactive alumina–LaPO<sub>4</sub> composite as machinable bioceramics

ABHISHEK BADOLIA, RITWIK SARKAR\* and SUMIT KUMAR PAL

Department of Ceramic Engineering, National Institute of Technology, Rourkela 769 008, Odisha, India

MS received 10 February 2015; accepted 17 March 2015

**Abstract.** Sintered Al<sub>2</sub>O<sub>3</sub>–LaPO<sub>4</sub> composites were prepared using commercially available reactive alumina and phase pure lanthanum phosphate (LP), prepared by the reaction synthesis technique. LP content was varied between 10 and 50 wt% and sintering was carried out between 1400 and 1600°C. Sintered composites were characterized for phase analysis, densification, strength, machinability, microstructure and bioactivity (in SBF solution) and biocompatibility (MTT assay protocol) studies. Composite nature was confirmed by phase analysis and LP was found to reduce the densification and strength values but imparted machinability. Again positive bioactivity and biocompatibility character were observed for all the compositions.

**Keywords.** Al<sub>2</sub>O<sub>3</sub>–LaPO<sub>4</sub> composite; densification; strength; machinability; bioactivity and biocompatibility studies.

### 1. Introduction

The revolution of human era, that fire can irreversibly transform clay into hard, fired ceramics (pottery) has resulted in a vast improvement in the quality and length of life. Similarly, the revolution occurred in ceramics to repair and reconstruct the damaged or diseased parts of the body/musculo-skeletal systems (the bioceramics),<sup>1</sup> has converted the concept of ceramic from a traditional clay-based material to a highly sophisticated functional material. Depending on their behaviour with biological environments, ceramics can be classified as bioinert, bioactive and bioresorbable materials. Bioinert ceramics, like alumina, have high compressive and bending strength and better biocompatibility compared with that of stainless steel. Due to better bioinert character and excellent mechanical features (low wear and high strength) alumina ceramics are used for osteosynthetic devices and joint prosthetics.<sup>2</sup> Alumina is also used in dentistry for better aesthetics and reliability of dental repair.<sup>3</sup>

Machining of ceramic is often required for the strict requirement of shape and dimensional control and high hardness of ceramics restricts the machining property through conventional techniques.<sup>4</sup> Thus requirement of costly diamond tools makes the machining of ceramics un-economical. In general, machinability refers to the easiness at which a material can be machined. Plenty of research work has been dedicated to improve the machinability of ceramics. Different approaches used to improve the machinability of

ceramics are, incorporation of weak interface phase material to create interfacial debonding, introduction of layered structure material in matrix to facilitate crack deflection and structure design method, where phase and porosity distribution in three dimension are controlled and optimized.<sup>4–6</sup> Generally rare earth phosphates (REP) such as LaPO<sub>4</sub> (LP), CePO<sub>4</sub> and YPO<sub>4</sub> in ceramic matrix (like Al<sub>2</sub>O<sub>3</sub> and ZrO<sub>2</sub>) impart and increase machinability by prolonging the crack route at the weak interfaces, causing inter-facial debonding and crack deflection between the two phases in a composite matrix,<sup>7–11</sup> where REPs act as a weak inter-phase in pure oxide systems.<sup>9</sup> Also increasing volume fraction of REPs was reported to increase the easiness of machining in ceramics.<sup>12</sup> In a fine-grained two-phase composite, material removal during machining occurs by the formation and linking of cracks at the weak interfaces between the alumina and REP phases.<sup>13</sup>

Lanthanum phosphate, monazite (LP) is an important REP suitable and effective as inter-phase material that exhibits high stability even at elevated temperatures in both oxidizing and reducing conditions and good chemical compatibility with oxide ceramics.<sup>14–16</sup> REPs are being used in biomedical fields, mainly as bio-imaging phosphor,<sup>17</sup> replacing the bioimaging organic fluorescent probes. Organic materials require ultra-violet (UV) excitation, which causes serious problem in bioimaging as it damages the biosystem and especially the organic fluorescent probe itself recognized as colour fading. The solution for UV damage on bioimaging system is the use of infra-red (IR) excitation and emission on rare earth compounds replacing organic compounds.<sup>18</sup> Rare earth orthophosphates, RPO<sub>4</sub> (LaPO<sub>4</sub> and Nd : LaPO<sub>4</sub>) have been studied for the application of bioimaging phosphor.<sup>19</sup> Lanthanide-based nanostructured inorganic phosphors

\*Author for correspondence (rite2badolia@rediffmail.com; ritwiksarkar@rediffmail.com)

(nanophosphors) are reported to be very useful for biochemical applications.<sup>20</sup> Use of up-converting nanoparticles based on rare earths for *in-vivo* imaging is also well studied.<sup>21–23</sup> Phosphor nanoparticles of 50–250 nm with up-converting properties were used to image the digestive system of the nematode *Caenorhabditis elegans* and reported that labelled individuals survive for days.<sup>24</sup> Also the viability of the rare earth-based phosphor nanoparticles for biological imaging was confirmed by imaging the digestive system of the nematode worm *C. elegans* and confirmed using energy-dispersive X-ray analysis that the up-conversion nanoparticles can be identified in a scanning electron microscope (SEM) at high spatial resolution.<sup>25</sup>

Such various uses of rare earth compounds in biomedical fields show their prospect also as weak inter-phase material in oxide ceramics. In the present work chemically synthesized  $\text{LaPO}_4$  was used as weak inter-phase material in the range of 10–50 wt% in alumina system. Sintered composites were prepared by pressing and sintering route and characterized for various properties including machinability by conventional drilling and bioactivity (immersing in SBF solution) and biocompatibility (MTT assay protocol) studies. Suitably developed such composites may be useful as biomedical implants in maxillofacial, dental and bone surgeries, where shape and dimensional criticality are important.

## 2. Experimental

### 2.1 Preparation of $\text{Al}_2\text{O}_3$ – $\text{LaPO}_4$ composites

LP powders were prepared according to the previous work<sup>26</sup> using the following chemical reaction and the process flow sheet is provided in figure 1. Phase purity of the calcined

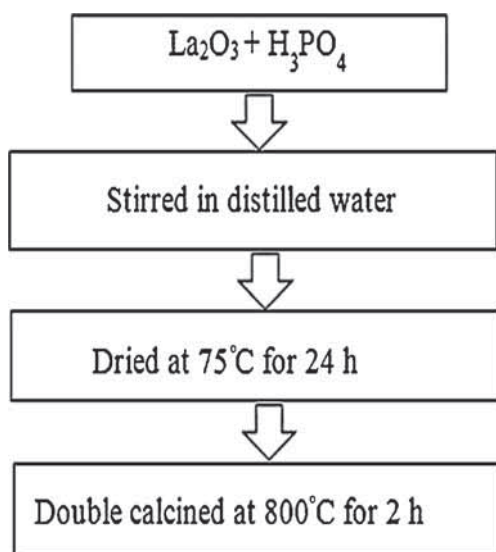
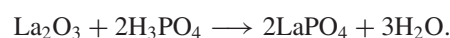


**Figure 1.** Flow sheet for preparation of lanthanum phosphate.

**Table 1.** Physico-chemical properties of alumina used.<sup>27</sup>

Properties	Alumina
$\text{Al}_2\text{O}_3$ (%)	99.8
$\text{Na}_2\text{O}$ (%)	0.07
$\text{Fe}_2\text{O}_3$ (%)	0.02
$\text{MgO}$ (%)	0.05
$\text{SiO}_2$ (%)	0.03
Specific surface area/BET ( $\text{m}^2 \text{g}^{-1}$ )	8.9
Average particle size, $D_{50}$ ( $\mu\text{m}$ )	0.4

powder was studied by powder X-ray diffraction (XRD) techniques.



Commercial grade high pure alumina (Almatis, India) was used for this study and the details are given in table 1.<sup>27</sup>  $\text{Al}_2\text{O}_3$ – $\text{LaPO}_4$  composites were prepared by the magnetic stirring method with different  $\text{LaPO}_4$  contents (10, 20, 30, 40 and 50 wt%) in wet (alcohol) medium for 1 h and then dried. The mixed powders were then pressed at 150 MPa in a hydraulic press (Carver, USA, make) to pellets (15 mm dia  $\times$  10 mm) and bar (60  $\times$  6  $\times$  6 mm) shapes using 4% PVA solution (6% concentration) as green binder and then sintered at 1400, 1450, 1500, 1550 and 1600°C with a soaking of 2 h in electrically heated programmable furnace (Bysakh, India, make).

### 2.2 Characterization of sintered composites

Sintered composites were characterized for phase analysis by powder XRD technique, using  $\text{Cu K}\alpha$  radiation through Ni filter, in an X-ray diffractometer (Rigaku, Japan make). Densitification study of the sintered samples was carried out by the liquid displacement method using Archimedes principle through vacuum method in water medium. Percent relative density was calculated as the ratio of bulk density to the theoretical density of each composition, taking the specific gravity of each component and their weight ratio used in the composition. Flexural strength of the sintered bars of each composition was calculated by using 3-point bending test in a universal testing machine (Tinius Olsen, USA, make). An average of five individual test results is represented as a data point in the study to make the plots of different experiments. Field-emission scanning electron microscope (FESEM) (FEI, USA, make) was used for the microstructure analysis of the fractured surface of the compositions. The machinability of the composites was tested using a conventional hand drill machine (Bosch, India, make) with a cemented carbide drill bit, 4 mm diameter at a speed of 450 rpm.

**Table 2.** Order and chemical composition of SBF solution.<sup>28</sup>

Order no.	Reagent	Amount (g)
1	NaCl	6.547
2	$\text{NaHCO}_3$	2.268
3	KCl	0.373
4	$\text{Na}_2\text{HPO}_4 \cdot 2\text{H}_2\text{O}$	0.178
5	$\text{MgCl}_2 \cdot 6\text{H}_2\text{O}$	0.305
6	$\text{CaCl}_2 \cdot 2\text{H}_2\text{O}$	0.368
7	$\text{Na}_2\text{SO}_4$	0.071
8	$(\text{CH}_2\text{OH})_3\text{CNH}_2$	6.057

### 2.3 Bioactivity and biocompatibility studies

**2.3a Simulated body fluid (SBF):** SBF is known to be metastable solution and having similar ion concentration as that of human plasma.<sup>28</sup> SBF solution was prepared by dissolving appropriate amounts of the chemicals in deionized water.<sup>29–32</sup> Details of the reagents used and their amounts are given in table 2. Sintered composites were immersed in SBF solution for 7 days in a humidified biochemical oxygen demand (BOD) incubator at 37°C and 90% humidity for bioactivity study. Growth of apatite crystals on the sintered composites was analysed by using FESEM.

**2.3b MTT assay:** The MTT assay study of the autoclaved sintered composites (powdered) was performed using MG-63 osteoblast cell line. The cells were maintained in Dulbecco's modified Eagle's medium (DMEM) with 10% FBS at 37°C, 5%  $\text{CO}_2$  and 95% humidity. The cells were seeded onto 96-well plate at a cell concentration of  $2 \times 10^4$  cells  $\text{ml}^{-1}$  and then incubated with the samples ( $50 \mu\text{g ml}^{-1}$ ) for 24 h. To detect the cell viability MTT working solution was prepared by diluting the stock solution (stock 5  $\text{mg ml}^{-1}$  PBS, pH 7.2) in growth medium without FBS to the final concentration of 0.8  $\text{mg ml}^{-1}$ . Briefly, 100  $\mu\text{l}$  of MTT working solution was added to each well and incubated for 4 h in  $\text{CO}_2$  incubator. After incubation, the media were removed carefully without disturbing formazan precipitate and dissolved in 100  $\mu\text{l}$  of 100% DMSO. An incubation for 15 min was done in dark and colourimetric estimation of formazan crystals was performed at 570 nm in a microplate reader.<sup>33</sup> Statistical analysis of the data was performed using two-way analysis of variance (ANOVA) to determine differences in cytotoxicity based on material ( $p < 0.05$ ).

## 3. Results and discussion

The physico-chemical properties of the starting alumina powder shows (table 1) that the alumina used is highly pure and fine.

### 3.1 Phase analysis study

Phase purity of the double calcined  $\text{LaPO}_4$  powder was confirmed by phase analysis by XRD which shows only LP phase with no other impurity phosphate or oxide phases (figure 2). Again, the  $\text{Al}_2\text{O}_3$ - $\text{LaPO}_4$  sintered products show only the reactant phases, namely corundum ( $\text{Al}_2\text{O}_3$ ) and lanthanum phosphate ( $\text{LaPO}_4$ ). This confirms that the reactant phases do not react within the composites for all the different contents of  $\text{LaPO}_4$  sintered at different temperatures.  $\text{Al}_2\text{O}_3$  and  $\text{LaPO}_4$  are present as separate phases at any amount of  $\text{LaPO}_4$  and  $\text{LaPO}_4$  remains as an interphase material in the alumina matrix. Phase analysis study of 10

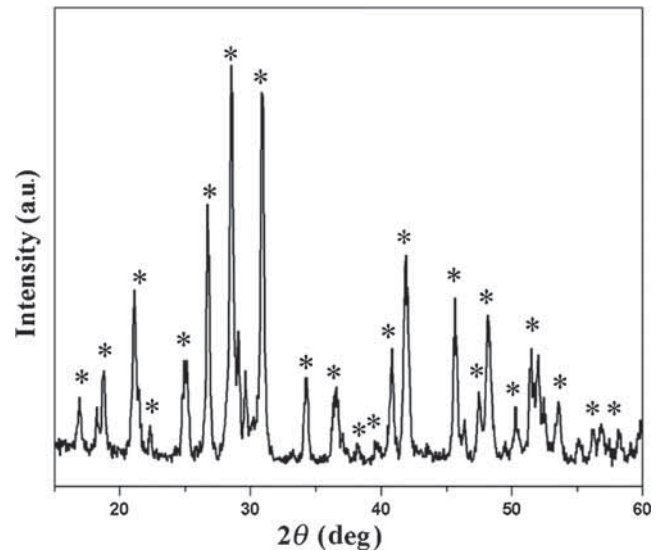


**Figure 2.** XRD pattern of calcined lanthanum phosphate. \* = lanthanum phosphate (32-0493).

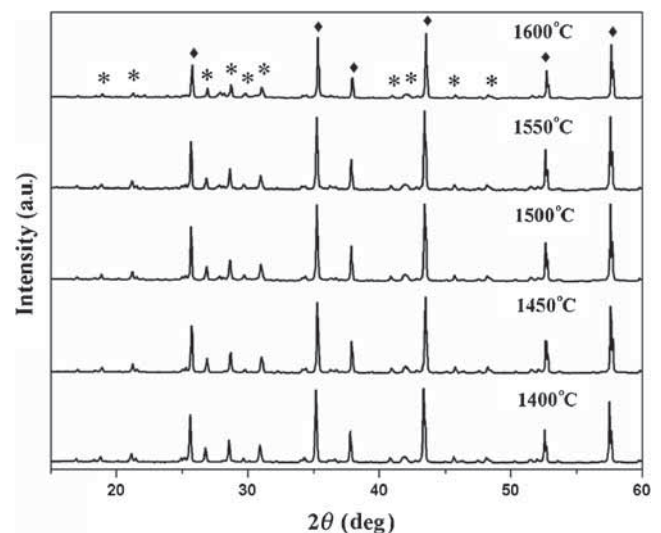


**Figure 3.** XRD pattern of 10 wt%  $\text{LaPO}_4$  containing composites sintered at different temperatures. \* =  $\text{LaPO}_4$  (32-0493); ♦ =  $\text{Al}_2\text{O}_3$  (42-1468).

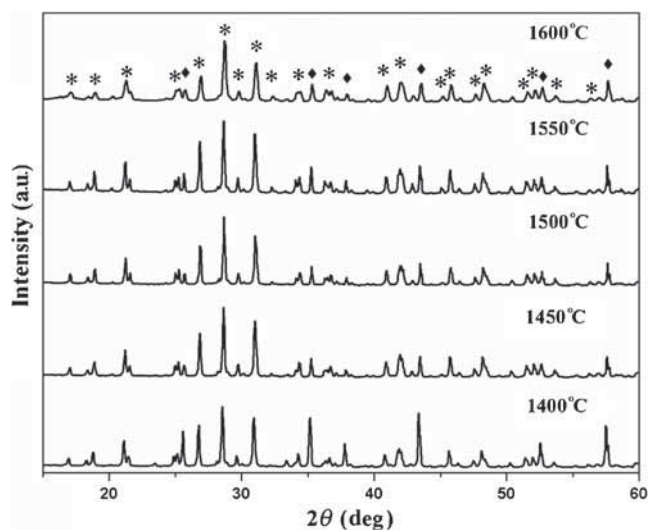


**Figure 4.** XRD pattern of 50 wt%  $\text{LaPO}_4$  containing composites sintered at different temperatures. \* =  $\text{LaPO}_4$  (32-0493); ♦ =  $\text{Al}_2\text{O}_3$  (42-1468).

and 50 wt% of  $\text{LaPO}_4$  containing composites sintered at different temperatures are shown in figures 3 and 4, respectively, as representative ones.

### 3.2 Densification and strength study

Increase in the sintering temperature has resulted in higher densification due to better sintering. However the addition of  $\text{LaPO}_4$  is found to reduce the extent of densification of the composites for all the sintering temperatures and increasing amount of  $\text{LaPO}_4$  is found to decrease the relative density continuously (figure 5).  $\text{LaPO}_4$  particles, present in between the alumina particles, act as a weak interphase material, results in interfacial debonding and reduced sintering/densification.<sup>9,12</sup> Although the bulk density values of the sintered samples were found due to increase in some cases due to higher specific gravity value of  $\text{LaPO}_4$ , but relative densification goes on decreasing with increasing amount of  $\text{LaPO}_4$ .

Variation of the flexural strength (figure 6) nearly follows the same trend as that found in densification studies. Increase in the sintering temperature increases the strength of composites may due to better densification at higher temperatures but increase in the amount of  $\text{LaPO}_4$  results in continuous decrease in the strength values, which is associated with desintering/debonding effect, as also observed in the densification behaviour.

### 3.3 Machinability of sintered composites

Drilling (machinability) study of pure alumina (without any  $\text{LaPO}_4$ ) shows complete cracking and breakage of the samples during drilling operation for all the different sintering temperatures (figure 7). Strong bonding of alumina does

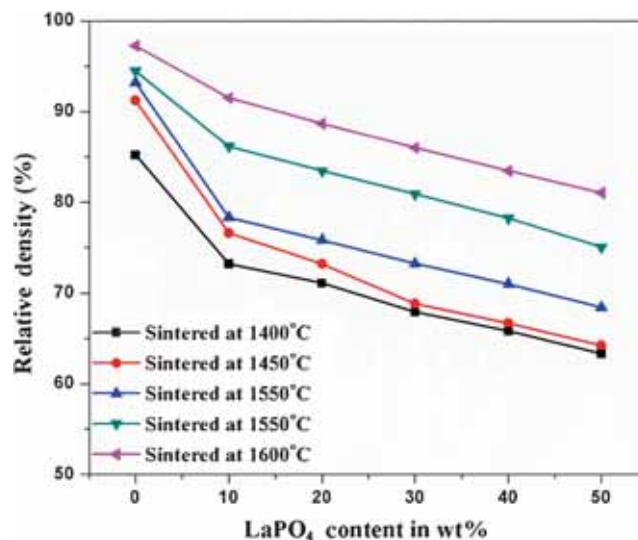


**Figure 5.** Relative density plot of  $\text{Al}_2\text{O}_3$ - $\text{LaPO}_4$  composites.

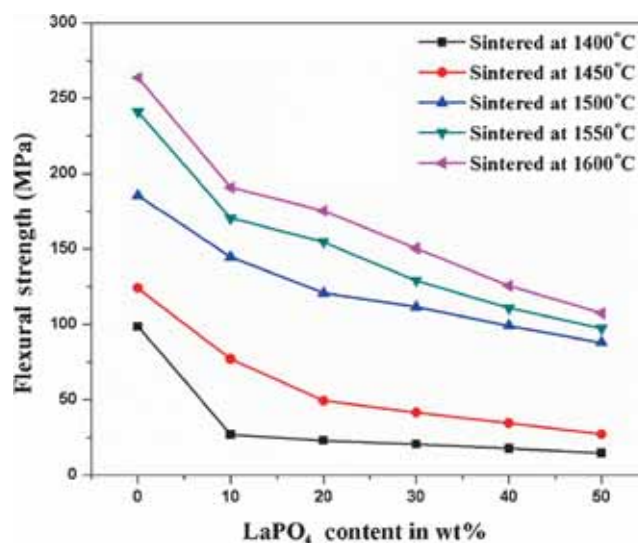


**Figure 6.** Flexural strength plot of  $\text{Al}_2\text{O}_3$ - $\text{LaPO}_4$  composites.

not allow the crack of drilling to propagate and brittle fracture occurs resulting in complete breakage of the samples. However the incorporation of  $\text{LaPO}_4$  in the alumina showed a completely different character (figure 8). Samples sintered at 1400, 1450 and 1500°C containing any amount of  $\text{LaPO}_4$  is drillable and smooth drilled surface was obtained, indicating easy machinable character of the sintered composites. For the composites sintered at 1550°C, a minimum of 20 wt% of  $\text{LaPO}_4$  and for composite sintered at 1600°C, minimum of 30 wt% of  $\text{LaPO}_4$  was found to be required to become drillable. This may be due to greater extent of densification of alumina at higher temperatures which is reducing the desintering and debonding effect of  $\text{LaPO}_4$  and requiring a threshold content for easy drillability. In general,  $\text{LaPO}_4$  is a fine and stable material which does not react with alumina even upto 1600°C and remains as weak interphase material, causing desintering and debonding in

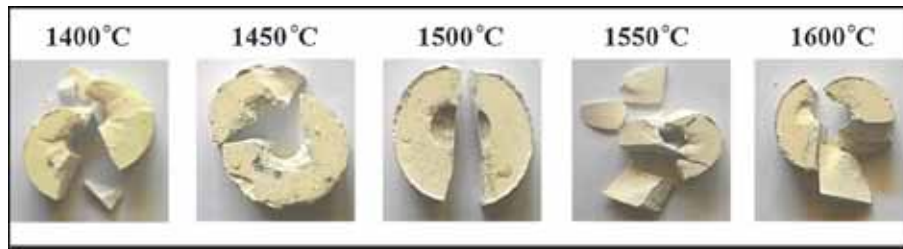


**Figure 7.** Photomicrographs of pure  $\text{Al}_2\text{O}_3$  sintered samples, after drilling operation.



**Figure 8.** Photographs of sintered  $\text{Al}_2\text{O}_3\text{-LaPO}_4$  composites after drilling.

alumina, deflects crack movement during machining and results in easy machinability. Also  $\text{LaPO}_4$  is distributed in the  $\text{Al}_2\text{O}_3$  matrix and refines the grain size of  $\text{Al}_2\text{O}_3$ ,<sup>4</sup> which helps in machinability.

### 3.4 Microstructure analysis

Microstructural developments of sintered  $\text{Al}_2\text{O}_3\text{-LaPO}_4$  composites with different  $\text{LaPO}_4$  contents are shown in figure 9. Lanthanum bearing phases appeared to be brighter in the field emission scanning electron microscopy (FESEM)

photomicrographs due to higher atomic number compared to that of aluminium. Microstructural photographs show that  $\text{LaPO}_4$  is well distributed among the alumina matrix, thus acting as a weak interphase material, causing de-sintering and debonding effect and resulting in crack deflection and machinability. Figure 9a–d shows the FESEM micrographs of the composites containing 10 and 50 wt%  $\text{LaPO}_4$  sintered at 1600°C as representative ones. Figure 9e shows the elementary distribution of different elements present in the system and indicates an overall uniform distribution of  $\text{LaPO}_4$  particles in alumina matrix.

### 3.5 Bioactivity and biocompatibility studies

Bioactivity of composites were investigated of the sample containing different ratios of  $\text{Al}_2\text{O}_3/\text{LaPO}_4$  (10–50 wt%) sintered at  $1600^\circ\text{C}$ . Sintered composites were found to be bioactive as the formation of apatite crystals were observed on immersion in SBF solution for 7 days. FESEM photomicrographs of the SBF-treated samples. Figure 10 confirms the formation of apatite crystals on the sintered surfaces of composites containing 10–50 wt% of  $\text{LaPO}_4$  and indicates the positive response of the composites in SBF bioactivity study.

The inverted microscope images and the cell viability index of cell incubation on composites after MTT assay analysis are shown in figures 11 and 12, respectively. The morphology of the cells were maintained with respect to control sample. Increasing amount of  $\text{LaPO}_4$  was found to affect the cell viability index and the same can also be observed in the inverted microscope image of cultured MG-63 fibroblast cell line after 24 h of incubation. However pure  $\text{LaPO}_4$  shows a viability of about 80 and 50%  $\text{LaPO}_4$  containing composite showed about 90% cell viability. This also proves that  $\text{LaPO}_4$  supported the growth of MG-63 osteoblasts. Hence this study proves that addition

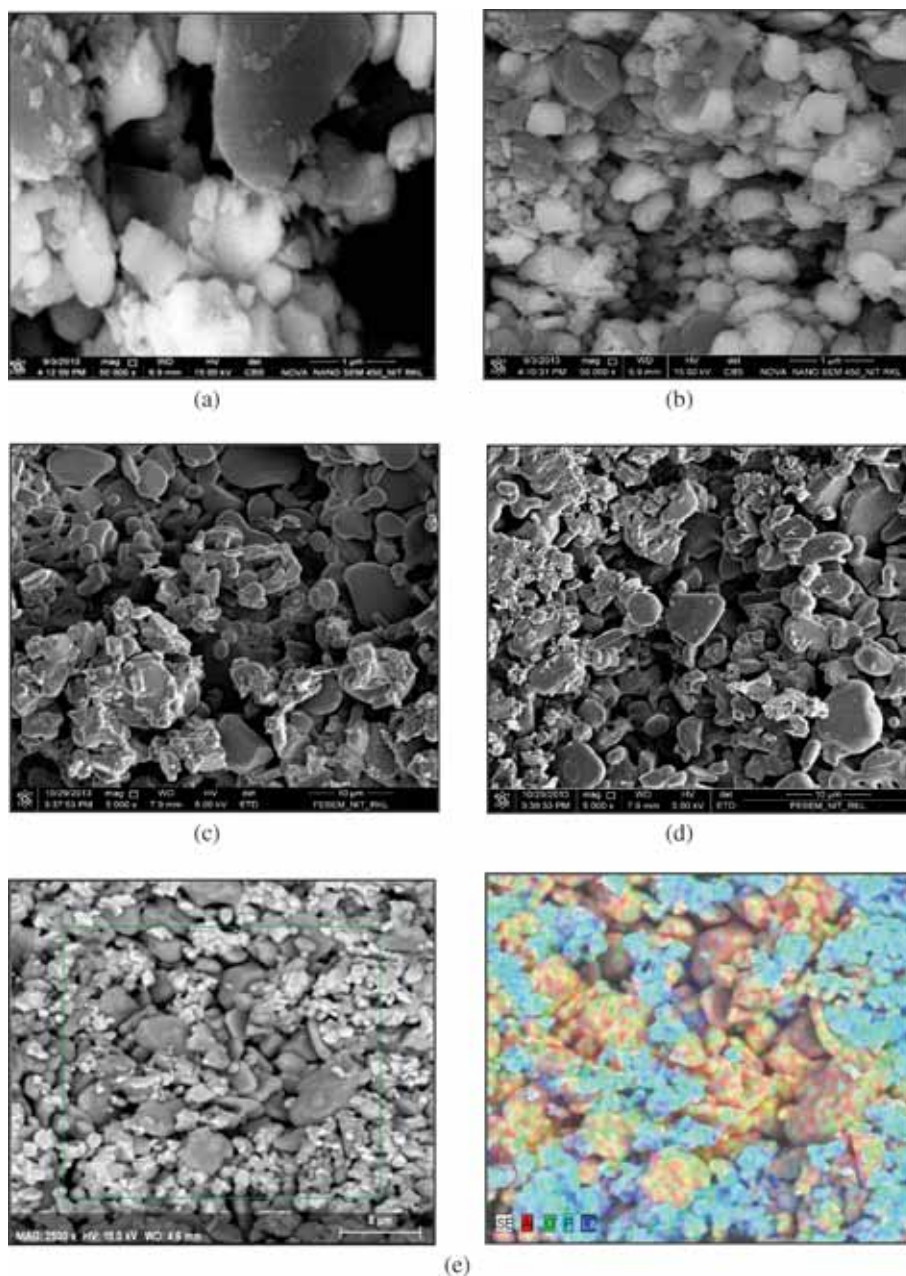


**Figure 9.** FESEM micrographs, sintered at  $1600^\circ\text{C}$ : (a) 10 wt% LP (back-scattered), (b) 50 wt% LP (back-scattered), (c) 10 wt% LP, (d) 50 wt% LP and (e) elementary mapping of 50 wt% LP.

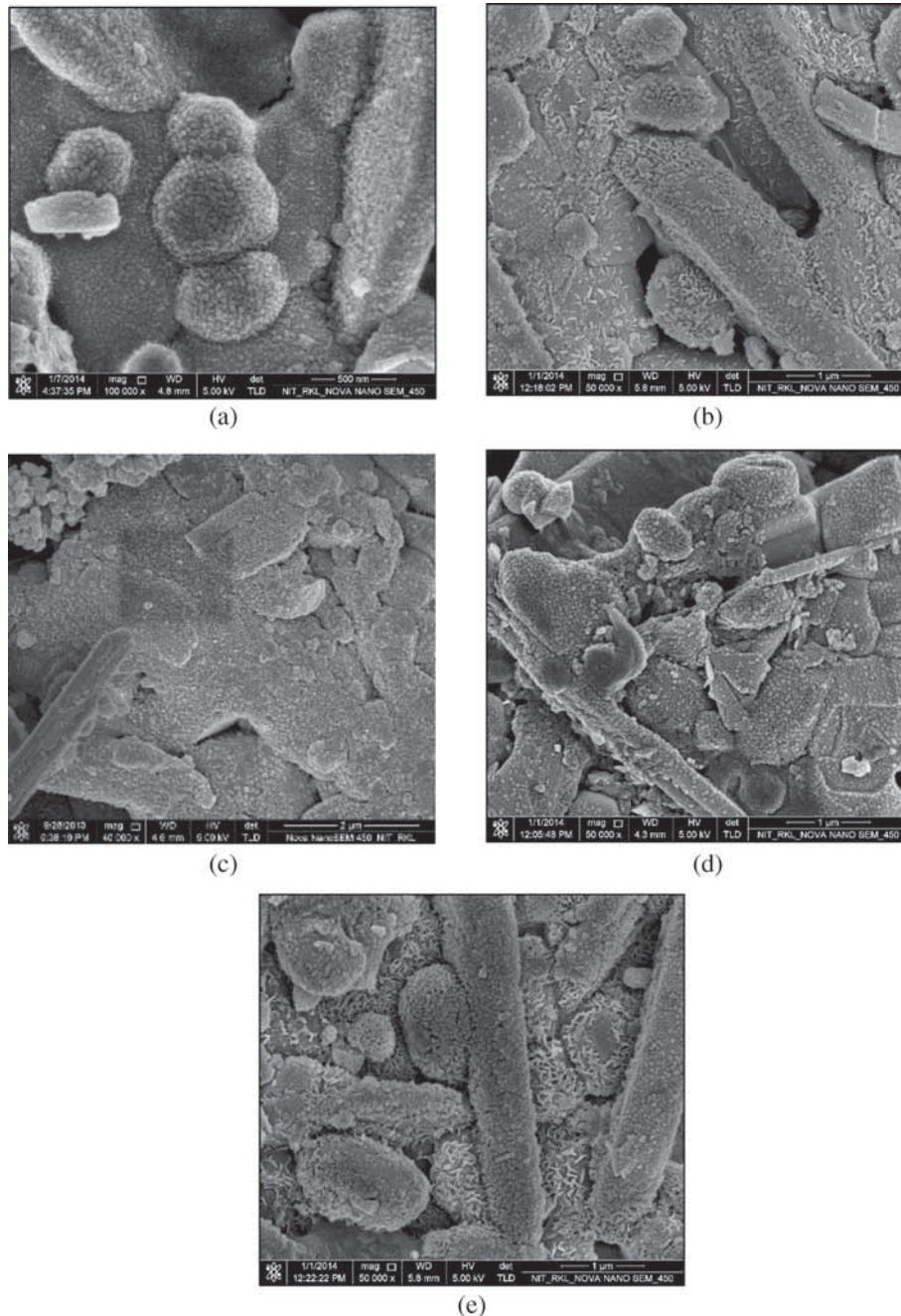


**Figure 10.** Growth of apatite crystals on the composite surface after 7 days in SBF: (a) 10 wt% of  $\text{LaPO}_4$ , (b) 20 wt% of  $\text{LaPO}_4$ , (c) 30 wt% of  $\text{LaPO}_4$ , (d) 40 wt% of  $\text{LaPO}_4$  and (e) 50 wt% of  $\text{LaPO}_4$ .

of  $\text{LaPO}_4$  to the composites is well suited for biomedical application.

#### 4. Conclusion

Phase pure  $\text{LaPO}_4$  was prepared using reaction synthesis route and was used to make  $\text{Al}_2\text{O}_3\text{-LaPO}_4$  composites. Free reactant phases and no reaction product were observed for the composites even on sintering at  $1600^\circ\text{C}$ . Relative density and flexural strength were found to be continuously

decreasing with the increase in the amount of  $\text{LaPO}_4$  content. Grossly all the  $\text{LaPO}_4$  containing composites were found to be drillable to conventional cemented carbide drill bit. Microstructural analysis showed well-distributed  $\text{LaPO}_4$  phase in the  $\text{Al}_2\text{O}_3$  matrix does not allow the material to densify, causing debonding effect resulting in improved machinability. Sintered  $\text{Al}_2\text{O}_3\text{-LaPO}_4$  composites also showed positive results for bioactivity in SBF solution and growth of apatite crystals. Also in biocompatibility study using MG-63 osteoblast cell line the composites showed high cell viability.

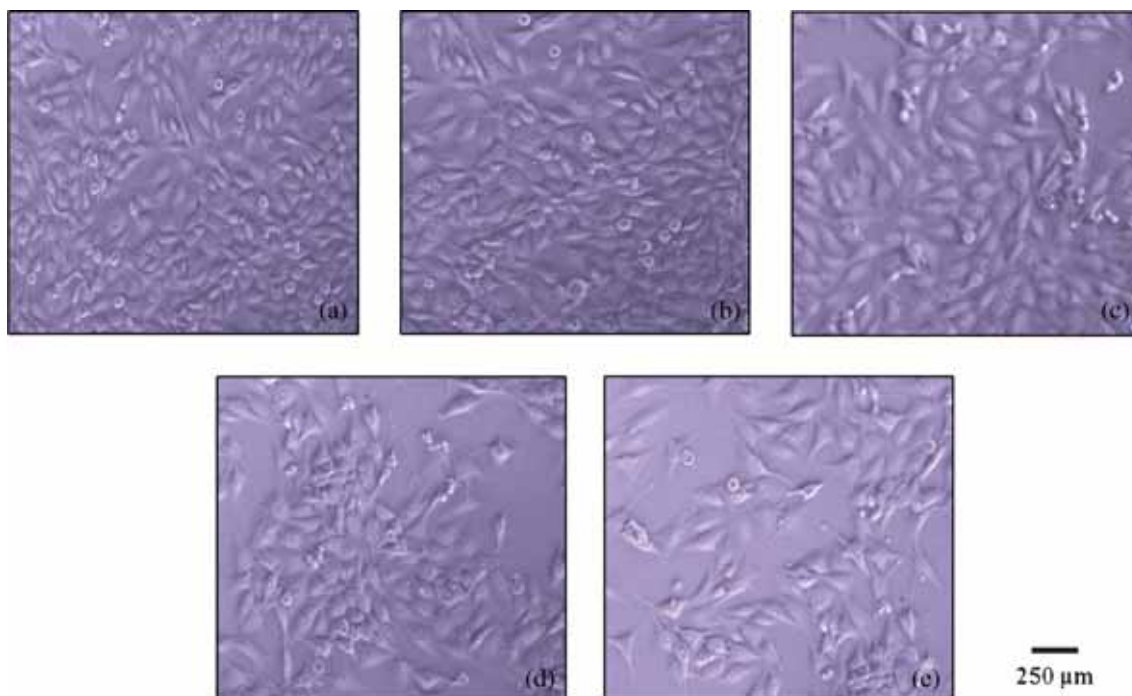


**Figure 11.** Inverted microscope image of cultured MG-63 fibroblast cell line after 24 h: (a) positive control, (b) pure  $\text{Al}_2\text{O}_3$ , (c) 10 wt% of  $\text{LaPO}_4$ , (d) 50 wt% of  $\text{LaPO}_4$  and (e) pure  $\text{LaPO}_4$ .

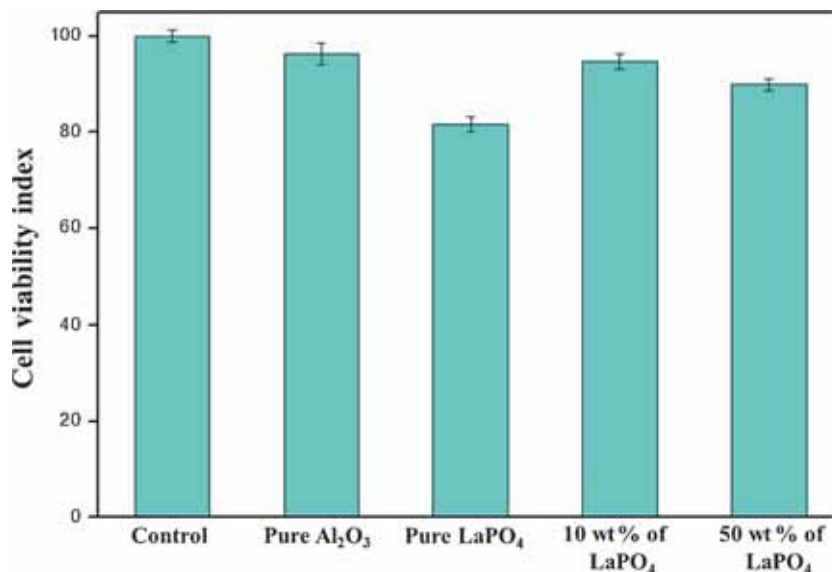


**Figure 12.** MTT assay of cells grown on control, pure  $\text{Al}_2\text{O}_3$ , pure  $\text{LaPO}_4$  and 10 wt% and 50 wt% of  $\text{LaPO}_4$ . Data represent the mean  $\pm$  SD for sample  $p < 0.05$  compared with control.

### Acknowledgements

We thankfully acknowledge the support of Almatris, India, for the alumina, Prof K Pal, Prof I Banerjee, Mr S Chakraborty of NIT, Rourkela, for their experimental support, Almatris India, for the support of alumina and staff of the Department of Ceramic Engineering, NIT, Rourkela, for their support in various experimentation of the work.

### References

1. Hench L L 1991 *J. Am. Ceram. Soc.* **74** 1487
2. Yamamura T, Kotoura Y, Kasahara K, Takahashi M and Abe M 1989 *Intraoperative radiotherapy and ceramic prosthesis replacement for osteosarcoma* (Tokyo: Springer Verlag).
3. Maccauro G, Iommetti P R, Raffaelli L and Manicone P F 2011 *Biomaterials applications for nanomedicine* (Chapter 15)



4. Wang R, Pan W, Chen J, Fang M and Meng J 2002 *Mater. Lett.* **57** 822
5. Grossman D G 1972 *J. Am. Ceram. Soc.* **55** 446
6. Pan W and Wang R G 2003 *Ceram. Int.* **29** 19
7. Min W, Daimon K, Matsubara T and Hikichi Y 2002 *Mat. Res. Bull.* **37** 1107
8. Zhou Z, Pan W and Xie Z 2003 *J. Euro. Ceram. Soc.* **23** 1649
9. Davis J B, Marshall D B, Housley R M and Morgan P E D 1998 *J. Am. Ceram. Soc.* **81** 2169
10. Kuo D H and Kriven W M 1998 *Mater. Sci. Eng. A* **241** 241
11. Davis J B, Marshall D B and Morgan P E D 1999 *J. Am. Ceram. Soc.* **19** 2421
12. Majeeda M A, Vijayaraghavan L, Malhotra S K and Krishnamorthy R 2009 *J. Mater. Proc. Technol.* **209** 2499
13. Morgan P E D, Marshall D B and Housley R M 1995 *Mater. Sci. Eng. A* **195** 215
14. Davis J B, Marshall D B and Morgan P E D 1999 *J. Eur. Ceram. Soc.* **19** 2421
15. Mawdsley J R, Kovar D and Halloran J W 2000 *J. Am. Ceram. Soc.* **83** 802
16. Davis J B, Marshall D B and Morgan P E D 2000 *J. Eur. Ceram. Soc.* **20** 583
17. Kodama N, Tanii Y and Yamaga M 2000 *J. Lumin.* **87-89** 1076
18. Kodama N, Sasaki N, Yamaga M and Masui Y 2001 *J. Lumin.* **94-95** 19
19. Byrappa K, Devaraju M K, Paramesh J R, Basavalingu B and Soga K 2008 *J. Mater. Sci.* **43** 2229
20. Dosev D, Nichkova M and Kennedy I M 2008 *J. Nanosci. Nanotechnol.* **8** 1052
21. Corstjens P L A M, Li S, Zuiderwijk M, Kardos K, Abrams W R, Niedbala R S and Tanke H 2005 *IEEE Proc.—Nanobiotechnol.* **152** 64
22. Kuningas K, Rantanen T, Karhunen U, Lovgren T and Soukka T 2005 *Anal. Chem.* **77** 2826
23. van, de Rijke F, Zijlmans H, Li S, Vail T, Raap A K, Niedbala R S and Tanke H J 2001 *Nat. Biotechnol.* **19** 273
24. Hope I A and Elegans C 1999 *A practical approach* (Oxford: Oxford University Press) 1st ed
25. Shuang F L, Robert R, William S R, Nora K, Chih-Kuan T, David T and Robert H A 2006 *Nano Lett.* **6** 169
26. Badolia A, Sarkar R and Pal S K 2014 *Trans. Ind. Ceram. Soc.* **73** 115
27. *Reactive alumina's for ceramic applications, Product catalogue* (USA: Almatris Inc.)
28. Tas C 2000 *Biomaterials* **2** 1429
29. Li P, Nakanishi K, de Groot K and Kokubo T 1994 *J. Am. Ceram. Soc.* **77** 1307
30. Li P, Nakanishi K, Kokubo T and de Groot K 1993 *Biomaterials* **14** 963
31. Cho S, Nakanishi K, Kokubo T, Soga N, Ohtsuki C, Nakamura T, Kitsugi T and Yamamuro T 1995 *J. Am. Ceram. Soc.* **78** 1769
32. Kokubo T, Miyaji F, Kim H M and Nakamura T 1996 *J. Am. Ceram. Soc.* **79** 1127
33. Ramirez P A, Romito A, Cosentino F and Milella E 2001 *Biomaterials* **22** 1467